

N72-29824

(NASA-CR-127459) PHOTOMETRIC STUDIES OF
SATURN'S RING AND ECLIPSES OF THE GALILEAN
SATELLITES Final Report W.E. Brunk (ITT
Research Inst.) 21 Apr. 1972 75 p CSCL 03B G3/30
Unclas 15576



CONTRACT NO. NASW-2257

FINAL REPORT

IITRI Project No. V6122

PHOTOMETRIC STUDIES OF SATURN'S RING
AND OF ECLIPSES OF THE GALILEAN
SATELLITES

Dr. William E. Brunk
Chief of Planetary Astronomy, Code SL
NASA Headquarters, FOB 6
Washington, D.C. 20546

Prepared by

M. J. Price
Astro Sciences
IIT Research Institute
10 West 35 Street
Chicago, Illinois 60616

21 April 1972

I

FINAL REPORT FOR CONTRACT NASW-2257 (IITRI NO. V6122)

PHOTOMETRIC STUDIES OF SATURN'S RING
AND OF ECLIPSES OF THE GALILEAN
SATELLITES

by

M.J. Price
Astro Sciences
IIT Research Institute
Chicago, Illinois 60616

for

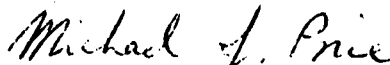
Dr. William E. Brunk
Chief of Planetary Astronomy, Code SL
NASA Headquarters, FOB 6
Washington, D. C. 20546

APPROVED BY:



C.A. Stone, Director
Physics Division

Respectfully submitted
IIT RESEARCH INSTITUTE



Michael J. Price
Associate Scientist
Astro Sciences

PHOTOMETRIC STUDIES OF SATURN'S RING AND OF ECLIPSES OF THE GALILEAN SATELLITES

1. INTRODUCTION

Contract NASW-2257 was awarded to IITRI on 1971 June 8 for photometric studies of Saturn's ring and of eclipses of Jupiter's Galilean satellites. Under the terms of the contract, IITRI would undertake a program to provide observations, data reduction and analysis related to the nature of Saturn's ring and to the composition of the Jovian atmosphere. For the Jovian atmospheric measurements, the recently developed Galilean satellite eclipse technique would be used to infer the optical scattering properties of the atmosphere. During three eclipses, occurring in 1971, photometry of the refraction tail of the ingress light curves would be performed in collaboration with Dr. John S. Hall at Lowell Observatory, Flagstaff, Arizona. For the photometric study of Saturn's ring, extensive library of calibrated photographs in the Planetary Research Center, Lowell Observatory would be used to determine a model of its physical structure. The mean apparent surface densities of particles in the two major components of the ring system (rings A and B) would be determined as part of the ring model. Dr. Michael J. Price would be the key personnel involved in the contract. The Period of Performance would be through 1972 May 7, with the Final Report due by 1972 June 7.

2. SATURN'S RING

Reliable data defining the photometric function of the Saturn ring system, at visual (V) wavelengths, have been interpreted in terms of a simple scattering model. Two classes of photometric data were used - observations of the phase effect, and measurements of the surface brightness of the ring system as a function of planetocentric solar declination angle (i.e., "tilt" angle). To facilitate the analysis, new photographic photometry of the ring was carried out utilizing the Lowell Observatory plate

collection. Homogeneous measurements of the mean surface brightness (rings A and B together), covering almost the complete range in tilt angle, were made. The ring model adopted was a plane-parallel slab of isotropically scattering particles; the single scattering albedo and the perpendicular optical thickness were both arbitrary. Results indicate that primary scattering is inadequate to describe the photometric properties of the ring; multiple scattering predominates for all angles of tilt with respect to the sun and Earth. In addition, the scattering phase function of the individual particles is significantly anisotropic; they scatter preferentially towards the sun. Minimum values for the single scattering albedo, and for the mean perpendicular optical thickness (rings A and B together) appear to be 0.90 and unity, respectively. On the basis of these results, all photometric ring models derived to date must be considered invalid. More thorough interpretation of the ring photometry in terms of the physical structure of the system is highly problematic, requiring the solution of a complex radiative transfer problem. At the present time, knowledge of the physical properties of the ring (including particle size information) is a completely open question. A preprint of a paper submitted to the Astronomical Journal is included as Appendix I.

3. ECLIPSES OF THE GALILEAN SATELLITES

Simultaneous two-color photometry of the Galilean satellites was carried out at blue ($\lambda 4500 \text{ \AA}$) and yellow ($\lambda 5790 \text{ \AA}$) wavelengths during their eclipses by Jupiter on 1971 March 10 (Ganymede) and on 1971 April 6 (Io and Europa). Observations were made using the Hall photometer attached to the 72-inch aperture reflector at Lowell Observatory.

For the Ganymede eclipse, the shape of the ingress light curve was reliably determined for extinctions up to 9 magnitudes in both colors. Neither curve showed any evidence of a refraction tail. The Jovian aerosol haze above the visible cloud

layer was essentially opaque. The observations have been interpreted in terms of the local optical transmission properties of the Jovian atmosphere. At gas number densities $\sim 5 \times 10^{18} \text{ cm}^{-3}$, the maximum photon scattering mean free path at visual wavelengths is 47 km atm. Evidence indicates that neither a simple reflecting layer model nor a semi-infinite, homogeneous scattering, haze model provides an adequate physical description of the atmosphere. Application of the eclipse technique in 1970 had shown that the atmosphere should be approximated by a vertically inhomogeneous scattering model; application in 1971 showed that the scattering mean free path is dependent on zenographic location and probably on time also. No unique scattering model exists for the Jovian atmosphere. Obvious profound implications arise, therefore, for the interpretation of Jovian spectra. Full details of the observations and their analysis will be published in the scientific literature; a preprint of the paper is attached (Appendix II).

For the Io and Europa eclipse, the seeing conditions did not permit accurate photometry of the refraction tail during ingress. Nevertheless, the observation data were sufficiently precise for new photometric radii for both satellites to be inferred. The results have been published in the Lowell Observatory Bulletin (No. 156, Vol. VII, No. 19, pp. 207-210); a copy is attached (Appendix III).

APPENDIX I

Preprint of paper entitled

"OPTICAL SCATTERING PROPERTIES OF SATURN'S RING"

by

M. J. Price

Submitted in 1972 April
for Publication in the

ASTRONOMICAL JOURNAL

OPTICAL SCATTERING PROPERTIES
OF
SATURN'S RING

Michael J. Price
IIT Research Institute
60 W. Giaconda Way
Tucson, Arizona 85704

Received _____

ABSTRACT

Reliable data defining the photometric function of the Saturn ring system at visual (V) wavelengths, are interpreted in terms of a simple scattering model. To facilitate the analysis, new photographic photometry of the ring has been carried out utilizing the Lowell Observatory plate collection. Homogeneous measurements of the mean surface brightness (rings A and B together), covering almost the complete range in planetocentric solar declination angle, are presented. The ring model adopted is a plane parallel slab of isotropically scattering particles; the single scattering albedo and the perpendicular optical thickness are both arbitrary. Results indicate that primary scattering is inadequate to describe the photometric properties of the ring; multiple scattering predominates for all angles of tilt with respect to the sun and Earth. In addition, the scattering phase function of the individual particles is significantly anisotropic; they scatter preferentially towards the sun. Minimum values for the single scattering albedo, and for the mean perpendicular optical thickness (rings A and B together) appear to be 0.90 and unity, respectively. Thorough interpretation of ring photometry in terms of the physical structure of the system is highly problematic, requiring the solution of a complex radiative transfer problem.

/

PRECEDING PAGE BLANK NOT FILMED

1. INTRODUCTION

Bobrov (1970) has recently reviewed current knowledge of Saturn's ring, paying particular attention to its historical development. Modern developments have been reviewed in more detail by Cook, Franklin, and Palluconi (1971). Both dynamical and photometric studies of the ring system have been made, but photometry provides the most direct technique for inferring its physical structure. Very few reliable photometric data exist, however, and their interpretation is uncertain. Deirmendjian (1969) has critically reviewed studies of the optical scattering properties of the ring.

Of the meagre observational data available, the most useful for studying the optical properties of the ring are quantitative measurements of its photometric function and qualitative estimates of its optical thickness. Unfortunately, the photometric function is incompletely defined, fairly extensive data being available only for visual (V) wavelengths. Measurements of the surface brightness of the ring system as a function of phase angle show a pronounced variation, the rings brightening dramatically at opposition. But the phase effect is poorly documented, reliable data existing for only one Saturn apparition, when the rings were wide open with respect to the sun and Earth. Surface brightness measurements as a function of planetocentric solar declination angle (i.e., the solar illumination angle, or "tilt" angle) have also been made. For constant phase angle, the surface brightness of the ring appears to vary slowly with the solar illumination angle. Because data are sparse, no useful information exists concerning the variation of the phase effect with tilt angle. Qualitative estimates of the transmission properties of the individual components of the ring system (rings A, B, and C) have been made from visual observations of several stellar occultations and of an eclipse of the satellite Iapetus. The mean perpendicular optical thickness of the ring system appears to be near unity.

Historically, the phase effect has been interpreted in terms of mutual shadowing among macroscopic ring particles. Interpretations have also been made using the Mie theory of

scattering, the small particles being either located individually within the ring or attached to the surfaces of much larger bodies. Explanations have been attempted in terms of shadowing within rough surface layers of macroscopic particles. Each interpretation has, however, been based on primary scattering alone. Multiple scattering among the individual particles has not been seriously considered even though observations of stellar occultations indicate that the ring is not optically thin.

Lumme (1970) has begun investigation of the role of multiple scattering in determining the photometric properties of the ring system. Interpreting the available data on the tilt effect in terms of an approximate radiative transfer theory, he concluded that multiple scattering is significant in both rings A and B for all solar illumination angles. For the single scattering albedo of the particles, he derived an optimum value of 0.90; values derived for the mean perpendicular optical thickness of rings A and B were 0.30 and 1.25, respectively. Although the analysis may be seriously questioned on the grounds that the meagre observational data were overinterpreted, the results remain provocative. If confirmed, photometric ring models derived to date are invalid.

In this paper, the role of multiple scattering is investigated further. Photometric data on both the phase and tilt effects are analyzed in terms of a simple scattering model. To facilitate the investigation, new photographic photometry of the tilt effect has been carried out.

2. OBSERVATIONAL DATA

2.1. Phase Effect

Reliable photoelectric/photographic photometry of the phase effect has been carried out by Franklin and Cook (1965). Accurate measurements of the apparent blue (B) and visual (V) magnitudes of Saturn's ring as a function of phase angle were made. Note, however, the important errata discussed by Cook, Franklin, and Palluconi (1971). The data cover almost the complete range in

phase angle (0° - 6°) accessible from Earth. During the course of the observations, the planetocentric declinations of the sun and Earth remained nearly constant near $-26(\pm 0.5)$ degrees. To facilitate the comparison of theory with observation, their visual photometric data were converted to intensity measurements. By means of standard photometric reduction techniques, values of I/F were derived, I being the mean specific intensity of the ring surface, and πF being the solar flux at Saturn. It was assumed that all light from the ring system is contributed by rings A and B, ring C making a negligible contribution. Separation of the individual contributions of rings A and B to the total brightness of the system was considered to be uncertain. Rings A and B were therefore treated together. Dimensions for rings A and B, and the apparent visual (V) magnitude of the sun, were taken from Allen (1963); geometrical information was obtained from The American Ephemeris and Nautical Almanac, 1959. I/F values were corrected to equal planetocentric declination angles of the sun and Earth using the method discussed in Section 3. The data were not, however, corrected to a constant solar illumination angle because its variation during the course of the observations was considered negligible. For convenience in the subsequent analysis, we will assume that the planetocentric declination of the sun was constant at the opposition value ($-26^{\circ}23'$). Final values for I/F , denoted I_0/F , are plotted as a function of phase angle α , in Fig.1.

2.2 Tilt Effect

Observational data defining the variation in the surface brightness of the Saturn ring system with planetocentric solar declination angle are meagre and imprecise. To date, only two sets of measurements, both based on photographic photometry alone, have been published. Camichel (1958) determined the surface brightness of each of the individual ring components, A and B, at visual (yellow) wavelengths for southerly planetocentric solar declinations in the range 3 - 26 degrees. But coverage was uneven and incomplete. During the 1966 Saturn apparition, Focas and Dollfus (1969) carried out a careful series of measurements at both blue and yellow wavelengths of the surface brightness of ring B. Both the sun and Earth passed individually through

the ring plane during the course of the observations. Planetocentric solar declination angles in the range ± 3 degrees were thoroughly covered. In both series of measurements, the intensities of the brightest regions of the ring components were derived using the center of the bright equatorial zone of the planet as a photometric standard. More accurate and homogeneous data are, however, required if a reliable theoretical interpretation is to be made. Accordingly, new measurements of the mean surface brightness of rings A and B together, covering the range in solar planetocentric declination angle of ± 26 degrees, have been made.

The Planetary Research Center, Lowell Observatory, Flagstaff, Arizona contains the largest, most complete, most homogeneous library of photometrically calibrated Saturn plates in existence. The Lowell collection is therefore ideally suited to a photographic photometric study of Saturn's ring. Until systematic observation of the planet was discontinued in 1965, calibrated plates were obtained at nearly every successive opposition beginning in 1924. The Saturn collection comprises over 350 multiple-image plates, almost all of which were secured by E.C. Slipher using the 24-inch aperture Lowell refractor. Slipher (1964) has published a summary of the results obtained in planetary photography at Lowell Observatory since 1904. Details of the observational procedures used are given, together with selected examples of the best photographs obtained. Undoubtedly, the collection of Saturn photographs is one of the finest in existence.

Of the 350 Saturn plates available, by far the majority (209) were exposed at visual (yellow) wavelengths through a Wratten No.12 filter, radiation in the range $\lambda\lambda 5000-5850\text{\AA}$ being recorded. Accordingly, the photometry was restricted to yellow wavelengths only. Typically 5-10 Saturn images are recorded on each plate, photometric calibration being provided by a step wedge. Plates were exposed for 1-3 seconds in order to record detail on the planetary disk. Consequently, only rings A and B are recorded, the crepe ring (C) being too faint. Except in 1939, the plate scale is constant at 4" arc/mm; in 1939, the scale is 8" arc/mm.

Plates were selected according to several criteria. Quality was most important. Plates whose emulsions showed signs of physical and chemical deterioration were rejected. So were poorly exposed plates, and those taken under bad seeing conditions. To minimize the photometric significance of the opposition effect, plates taken at phase angles less than 1.5 degrees were not used. Measurements of ring brightness could be made except when the ring was nearly edge-on. Seeing effects and scattered light from the planet prevented reliable photometry when the planetocentric declination of the Earth was less than 2 degrees. Even so, sufficient plates (61) were selected to provide very satisfactory coverage in planetocentric solar declination angle.

Standard photographic photometric procedures were used in the analysis of the plates. A Joyce-Loebl Automatic Recording Microdensitometer Model Mk.IIIC was used to scan the best image on each plate. In every case, the scan was made along the major axis of the ring system, the spot passing over both ansae and the disk of the planet. To resolve Cassini's division, the scanning spot was a 100- μ square, equivalent to a 0".4 square on a typical plate. Smaller scanning apertures, although desirable for better spatial resolution, produced an unacceptable level of photographic grain noise in the tracings. Fig.2 illustrates some of the data.

Digitization of each density tracing was carried out for a spatial interval corresponding to an angular resolution 0".4 arc. The characteristic curve for each plate was defined, typically, by four calibration wedge steps, separated in density by successive factors of 2. After density-intensity conversion, the digitized data were used to derive the quantity I_R/I_P , where I_R is the mean specific intensity of the ring surface and I_P is the mean intensity of Saturn's disk. The intensity profiles of both ansae were averaged to derive the radial intensity of the ring system. Mean intensities for both the ring and the disk were then derived by area-weighting each profile. Both the ring and disk were assumed to be radially symmetric, the oblateness of Saturn being neglected. Because the

plates did not record the crepe ring, I_R/I_P is a measure of the mean specific intensity of rings A and B together.

Table I summarizes the results. Column 1 identifies each plate according to date, color, and time. For example, the plate taken on 1924 July 30, through the yellow Wratten No.12 filter, at 03^h18^m Universal Time, has the identification 24 07 30 Y 03:18. Columns 2 and 3 list the planetocentric declination angles of the sun (D_S) and Earth (D_E), respectively. Saturn's phase angle (α) is given in column 4. All three are measured in degrees. Column 5 lists I_R/I_P . Finally, in column 6, the quality index of the plate, subjectively assessed on a scale 1-3, usable -best, is noted. Quality index provides a coarse estimate of the atmospheric seeing conditions at the time of exposure. If the quality index is unity, Cassini's division is barely resolved, the diameter of the seeing disk being $\sim 1''$ arc. Plates having quality indices 3 were exposed under very superior seeing conditions. In those cases, when the ring is open, Cassini's division is very clearly resolved. Indeed, from the sharpness of the interior and exterior edges of the division on the microdensitometer tracings, the diameter of the seeing disk must then have been $\sim 0.2''$ arc.

Because of the method used to analyze the photographic data, systematic errors may affect the derived I_R/I_P values. Such errors can result from changes in the distribution of reflectivity over Saturn's disk, and from neglect of the planet's oblateness. Random errors are generated during the standard photometric reduction procedure.

Present knowledge of the brightness distribution over the disk of Saturn has been reviewed by Alexander (1962). At visual (yellow) wavelengths, the planet generally shows a bright equatorial zone, alternating series of narrow zones and belts at temperate latitudes, and darker polar regions. Pronounced limb-darkening is always apparent. Significant temporal changes in the latitudinal distribution of surface brightness have been observed; variation in the prominence of the equatorial zone is the most striking. Harris (1961) has reviewed Saturn photometry covering the time frame 1862-1952 to determine if there are

any significant long-term variations in the reflectivity of its integrated disk. None approaching even 5 percent was found. Harris also noted that any short-period variations with rotational phase are probably very small (~1 percent).

Neglecting the latitudinal distribution of reflectivity over Saturn's disk causes the ring brightness to be underestimated, the mean intensity of the disk being overestimated because too much weight is given to the equatorial zone. In principle, use of a polar scan in the analysis rather than an equatorial scan would permit a better estimate to be made of the mean intensity of the planetary disk. In practice, however, the quality of the photometric data did not warrant the additional sophistication. By comparison, neglecting the oblateness of Saturn has a decidedly second-order effect on derivation of the ring brightness.

To obtain a conservative estimate for the systematic effect resulting from the latitudinal distribution of reflectivity over the planetary disk, the photographic plate (Table I, #41 12 09 Y 01:23) showing the most prominent equatorial zone was re-analyzed using both polar and equatorial scans (cf. Fig. 3). Mean disk intensities were derived from both scans, their polar/equatorial ratio being 0.837. On the basis of this result, the relative accuracy of the photographic photometry was estimated to be ± 10 percent. Support for this estimate comes from an empirical study of Table I for temporal effects. Ring brightness measurements made under similar geometrical conditions, but in different years, were consistent within the same relative accuracy.

Random errors, although not negligible, are less significant. Such errors arise primarily from uncertainties in defining the precise shape of the characteristic curve for each plate. Their magnitude may be estimated from Table I also. Measurements made from individual plates taken on the same night have an average rms error ~3 percent. Short-term variations in the surface brightness of Saturn's disk must be small; measurements made on adjacent nights are consistent within the single night rms error.

To facilitate theoretical study of the variation of the surface brightness of the ring system with solar illumination angle, the I_R/I_P determinations have been converted to I/F values, corrected to a constant phase angle. Two phase angles are used for reference. I/F values corrected to zero phase are denoted I_1/F . Those corrected to a phase angle of 6 degrees are labelled I_2/F . Corrections were made using phase information on the ratio of the ring and integrated disk brightnesses presented by Franklin and Cook (1965) after revision for the errata discussed by Cook, Franklin, and Palluconi (1971). Minor extrapolations of the information to phase angles of zero and six degrees were not difficult. Because of lack of data to the contrary, we have assumed that the phase effects apparent in Franklin and Cook's disk and ring photometry do not vary with solar illumination angle. I_1/F values were obtained from the relation

$$\frac{I_1}{F} = p(V) \frac{I'_R}{I'_P} \quad (1)$$

where $p(V)$ is the geometrical albedo of Saturn's disk at visual (V) wavelengths, and I'_R/I'_P corresponds to I_R/I_P corrected to zero phase angle. For $p(V)$, we have adopted the value given by Irvine and Lane (1971). Values of I_1/F derived from equation (1) have been corrected to equal planetocentric declinations of the sun and Earth using the method discussed in Section 3. I_2/F values were obtained by scaling the resultant I_1/F values according to Fig.1. The results are plotted in Fig4. Both I_1/F and I_2/F ordinate scales are used; the abscissa μ_0 is the cosine of the angle of incidence or reflection with respect to the outward normal to the ring surface.

Photometry of the phase and tilt effects may be quantitative compared when the geometrical configuration of the sun, Saturn, and Earth was similar. Values of I_0/F at phase angles of zero and six degrees should agree with values of I_1/F and I_2/F corresponding to μ_0 equal to 0.442 (i.e., $\sin 26^\circ 23'$). Bearing in mind the accuracy of the photometry, the agreement is satisfactory.

3. RING MODEL

As a basis for discussion, the ring system is assumed to be an horizontally infinite, homogeneous, plane-parallel slab of isotropically scattering particles. Both the single scattering albedo ($\tilde{\omega}$) and the perpendicular optical thickness (τ) are considered arbitrary. Sunlight illuminating the ring may be represented by a parallel beam of radiation of net flux πF per unit area normal to itself. Chandrasekhar (1950) has obtained the exact solution of the corresponding multiple scattering problem. In Chandrasekhar's notation, the specific intensity of diffusely scattering radiation may be written

$$I(0; \mu) = (1/4) \tilde{\omega} F \frac{\mu_0}{\mu + \mu_0} [X(\mu)X(\mu_0) - Y(\mu)Y(\mu_0)] \quad (2)$$

where μ_0 and μ are, respectively, the direction cosines of the angles of incidence and reflection with respect to the outward normal to the ring plane. In the limiting case where $\tau \rightarrow \infty$,

$$X(\mu) \rightarrow H(\mu) \quad \text{and} \quad Y(\mu) \rightarrow 0. \quad (3)$$

In the special case where primary scattering alone need be considered (i.e., $\tau \rightarrow 0$),

$$X(\mu) \rightarrow 1 \quad \text{and} \quad Y(\mu) \rightarrow e^{-\tau/\mu}. \quad (4)$$

Numerical values for Chandrasekhar's X-, Y-, and H-functions have been tabulated for wide ranges of the parameters τ and $\tilde{\omega}$ by Carlstedt and Mullikin (1966).

Since Saturn and Earth move in nearly co-planar orbits, with the phase angle always remaining small, photometric observations of the ring always correspond to the case where the angles of incidence and reflection are nearly equal; the inclination of Saturn's orbit to the ecliptic is 2.5 degrees, while the phase angle is never more than 6 degrees. At opposition, the angles of incidence and reflection never differ by more than ± 2.5 degrees. To simplify comparison of theory with observation, the photometric data are corrected to the special case of equal angles of incidence and reflection; such corrections are significant when μ_0 and μ are small.

Specific intensities derived from equation (2) for unequal angles of incidence and reflection may be readily related to those corresponding to equal angles. Because the X- and Y-functions do not vary drastically with μ , we can write

$$X(\mu)X(\mu_0) - Y(\mu)Y(\mu_0) = X^2(\mu_0) - Y^2(\mu_0). \quad (5)$$

Numerical experiments with the Carlstedt and Mullikin tables indicate that equation (5) is valid to an accuracy ~ 5 per cent or better for ring parameters in the ranges $0.4 \leq \tilde{\omega} \leq 1.00$, $0.2 \leq \tau \leq \infty$, $0.0 \leq \mu \leq 0.5$, where $|\mu - \mu_0| \leq 0.04$. Substituting equation (5) into equation (2),

$$I(0, \mu) = (1/4) \tilde{\omega} F \frac{\mu_0}{\mu + \mu_0} [X^2(\mu_0) - Y^2(\mu_0)]. \quad (6)$$

But, when μ and μ_0 are equal, equation (2) becomes

$$I(0, \mu_0) = (1/8) \tilde{\omega} F [X^2(\mu_0) - Y^2(\mu_0)]. \quad (7)$$

Combining equations (6) and (7), we have

$$I(0, \mu_0) = (1/2) [1 + \mu/\mu_0] I(0, \mu). \quad (8)$$

To a good approximation, ring photometric data corrected to zero phase angle may be adjusted to the case of equal angles of incidence and reflection using equation (8).

Fig.4 summarizes theoretical calculations of $I(0, \mu_0)/F$ as a function of μ_0 for values of $\tilde{\omega}$ and τ in the ranges $0.6 \leq \tilde{\omega} \leq 1.00$, $0.2 \leq \tau \leq \infty$. Values of $I(0, \mu_0)/F$ were computed for the general case of multiple scattering using equation (7). For each value of $\tilde{\omega}$, the additional special case of primary scattering alone ($\tau = 0.5$) was computed.

4. DISCUSSION

Qualitative and quantitative comparisons between theory and observation can be made from Figs. 1, 4, and 5. On the basis of the scattering model, several conclusions can be drawn. First, the phase effect (Fig.1) is clearly a manifestation of the scattering phase function of the individual ring particles; isotropic

scattering will not produce a phase effect. Moreover, not only must the ring particles scatter anisotropically, but preferentially towards the sun. Second, primary scattering is insufficient to account for the tilt effect (Fig.4). Equations (4) and (6) indicate that $I(0, \mu_0)$ would then decrease monotonically with increasing μ_0 ; the observed trend is in the opposite sense. Multiple scattering must, therefore, predominate for all solar illumination angles. Third, the individual ring particles must be highly efficient scatterers. Minimum values for τ and $\tilde{\omega}$ appear to be unity and 0.90, respectively.

It might be argued that Fig.4 does not reliably depict the tilt effect, because the plotted data depend on our assumption regarding the invariability of the phase effect. Because the phase effect results from the anisotropic phase function of the ring particles, multiple scattering will cause it to become progressively less pronounced as the solar illumination angle decreases. But, even if the phase effect disappeared entirely at the lowest planetocentric solar declination angles, the trend of Fig.4 would persist.

5. CONCLUDING REMARKS

Our results indicate that theoretical interpretation of Saturn ring photometry in terms of the physical properties of individual particles is highly problematic, requiring the solution of a complex radiative transfer problem. There is a distinct need for higher quality, more extensive, data in the analysis. A long-term photoelectric observational program to completely define the photometric function of the ring system should be carried out.

Acknowledgements

It is a pleasure to thank W.A.Baum, Director of the Planetary Research Center, Lowell Observatory for his hospitality. Thanks are due also to Mr. Stuart Jones and Miss Sharon A.Konen, respectively, for technical assistance in the microdensitometry of the photographic plates, and in the reduction and analysis of the data. This research was sponsored by the National Aeronautics and Space Administration under contract NASW-2257.

REFERENCES

- Alexander, A.F. O'D. (1962) "The Planet Saturn", Faber and Faber, London.
- Allen, C.W. (1963) "Astrophysical Quantities", Athlone, London.
- Bobrov, M.S. (1970) in "Surfaces and Interiors of Planets and Satellites" ed. A. Dollfus, Academic, London, p.377.
- Camichel, H. (1958) Ann.d'Astrophys. 21, 231.
- Carlstedt, J.L. and Mullikin, T.W. (1966) Ap.J. Suppl. Series No.113, v.XII, p.449.
- Chandrasekhar, S. (1950) "Radiative Transfer", Oxford.
- Cook, A.F., Franklin, F.A. and Palluconi, F.D. (1971) "Saturn's Rings-A Survey", JPL Tech.Memorandum 33-488.
- Deirmendjian, D. (1969) "Electromagnetic Scattering on Spherical Polydispersions", Elsevier, New York, p.134.
- Focas, J.H. and Dollfus, A. (1969) Astron.Astrophys. 2, 251.
- Franklin, F.A. and Cook, A.F. (1965) Astron.J. 70, 704.
- Harris, D.L. (1961) in "Planets and Satellites, ed. G.P.Kuiper, and B.M. Middlehurst, Univ.of Chicago Press, p.282.
- Irvine, W.M. and Lane, A.P. (1971) Icarus, 15, 18.
- Lumme, K. (1970) Astrophys.Spa.Sci. 8, 90.
- Slipher, E.C. (1964) "A Photographic Study of the Brighter Planets" ed. J.S.Hall, Northland Press, Flagstaff, Arizona.

FIGURE CAPTIONS

Fig.1. Observations of the Saturn ring phase effect at visual (V) wavelengths; values of I_0/F versus α . I_0 is the mean specific intensity of the ring surface (rings A and B together), corrected to equal angles of incidence and reflection; πF is the solar flux at Saturn; α is the phase angle. Throughout, the planetocentric solar declination angle was essentially constant at the opposition value, $-26^\circ 23'$.

Fig.2. Equatorial microdensitometer scans of two Saturn plates from the Lowell Observatory collection (see, Table I). Plate #36 10 13 Y 05:10 was taken when the ring system appeared nearly edge-on; plate # 41 10 11 Y 11:50, when nearly wide open. Raw density profiles are shown.

Fig.3. Polar and equatorial microdensitometer scans of the Saturn plate taken at Lowell Observatory on 1941 December 9 at 01:23 U.T. Raw density profiles are shown.

Fig.4. Observations of the Saturn ring tilt effect at visual (V) wavelengths; values of I/F versus μ_0 . I is the mean specific intensity of the ring surface (rings A and B together), corrected to equal angles of incidence and reflection; πF is the solar flux at Saturn; μ_0 is the cosine of the angle of incidence with respect to the outward normal. Two ordinate scales are used. I_1/F values refer to zero phase; I_2/F values refer to a phase angle of six degrees. I_1 and I_2 are related through the phase curve given in Fig.1.

Fig. 5. Theoretical values of $I(0, \mu_0)/F$ versus μ_0 for an isotropically scattering ring model with parameters covering the range $0.60 \leq \tilde{\omega} \leq 1.00$, $0.2 \leq \tau \leq \infty$; $I(0, \mu_0)$ is the specific intensity of the ring surface; πF is the solar flux at Saturn; μ_0 is the cosine of the angle of incidence and reflection with respect to the outward normal; $\tilde{\omega}$ and τ are, respectively, the single scattering albedo and the perpendicular optical thickness. Solid curves show the general case of multiple scattering; each is labelled according to the τ value. Dotted curves show the case of primary scattering alone for $\tau = 0.5$.

TABLE I

SATURN RING PHOTOMETRIC DATA; LOWELL OBSERVATORY PHOTOGRAPHIC PLATES

PLATE	D_S	D_E	α	I_R/I_P	QUALITY
24 07 30 Y 03:18	+16.7	+14.6	5.9	0.784	2
25 07 24 Y 03:00	+20.5	+18.7	5.9	0.689	3
25 07 24 Y 03:10	+20.5	+18.7	5.9	0.731	2
25 08 08 Y 03:05	+20.6	+18.9	5.9	0.760	2
25 08 08 Y 03:15	+20.6	+18.9	5.9	0.812	2
28 08 04 Y 03:44	+26.6	+26.4	5.0	0.714	2
31 06 24 Y 08:30	+23.7	+23.2	1.9	0.834	1
31 09 08 Y 02:50	+23.2	+24.5	4.9	0.728	2
31 09 27 Y 02:30	+23.0	+24.5	5.6	0.687	2
32 11 30 Y 01:15	+19.3	+20.9	4.6	0.585	2
33 08 28 Y 06:27	+16.4	+17.4	2.3	0.767	3
33 08 29 Y 02:55	+16.4	+17.5	2.4	0.742	2
33 08 29 Y 03:13	+16.4	+17.5	2.4	0.724	2
33 08 29 Y 04:02	+16.4	+17.5	2.4	0.768	2
33 08 29 Y 05:09	+16.4	+17.5	2.4	0.737	2
33 08 29 Y 05:25	+16.4	+17.5	2.4	0.754	2
33 08 30 Y 06:26	+16.4	+17.5	2.5	0.742	2
33 08 30 Y 08:19	+16.4	+17.5	2.5	0.703	1
33 08 31 Y 07:34	+16.4	+17.5	2.6	0.716	2
33 08 31 Y 07:46	+16.4	+17.5	2.6	0.747	2
33 08 31 Y 08:29	+16.4	+17.5	2.6	0.787	2
33 09 05 Y 07:51	+16.3	+17.6	3.0	0.669	2
33 09 10 Y 06:52	+16.3	+17.7	3.5	0.623	3
33 09 12 Y 04:35	+16.3	+17.8	3.6	0.607	2
33 09 12 Y 04:58	+16.3	+17.8	3.6	0.643	2
33 09 12 Y 06:28	+16.3	+17.8	3.6	0.712	2
33 09 14 Y 06:28	+16.2	+17.8	3.8	0.730	2
33 09 16 Y 04:57	+16.2	+17.9	3.9	0.718	2
33 09 22 Y 04:40	+16.2	+17.9	4.4	0.738	2
33 09 22 Y 05:04	+16.2	+17.9	4.4	0.736	2
33 09 25 Y 03:12	+16.1	+18.0	4.5	0.647	2
33 09 27 Y 04:03	+16.1	+18.0	4.7	0.729	2
34 09 19 Y 04:34	+11.7	+13.2	3.2	0.676	3

TABLE I (cont'd)

PHOTOMETRIC DATA

PLATE	D_S	D_E	α	I_R/I_P	QUALITY
35 06 06 Y 11:22	+08.3	+05.5	6.0	0.696	2
35 06 06 Y 11:43	+08.3	+05.5	6.0	0.676	2
35 06 07 Y 11:35	+08.2	+05.5	5.9	0.737	2
35 10 01 Y 03:10	+06.6	+08.2	3.2	0.598	3
36 10 13 Y 05:10	+01.1	+02.8	3.2	0.238	3
37 07 16 Y 10:10	-03.0	-05.6	5.8	0.423	2
37 07 17 Y 11:21	-03.0	-05.6	5.8	0.404	3
39 10 01 Y 08:39	-14.7	-15.3	2.3	0.752	1
39 12 06 Y 06:19	-15.6	-13.7	4.5	0.780	1
39 12 06 Y 06:31	-15.6	-13.7	4.5	0.770	1
39 12 07 Y 05:28	-15.6	-13.7	4.6	0.756	1
39 12 08 Y 05:37	-15.6	-13.6	4.7	0.732	2
39 12 08 Y 06:10	-15.6	-13.6	4.7	0.805	1
39 12 08 Y 06:21	-15.6	-13.6	4.7	0.852	1
40 10 18 Y 10:09	-19.5	-19.8	1.9	0.798	3
41 10 07 Y 12:35	-23.1	-23.8	4.4	0.705	3
41 10 11 Y 11:50	-23.2	-23.8	4.0	0.725	3
41 12 09 Y 01:23	-23.7	-22.9	2.4	0.788	3
43 11 11 Y 07:59	-26.8	-26.5	3.8	0.746	2
45 11 29 Y 08:30	-23.7	-22.3	4.6	0.786	3
50 02 16 Y 08:35	-03.4	-02.6	2.1	0.490	3
50 02 16 Y 10:54	-03.4	-02.6	2.1	0.558	3
52 04 17 Y 06:09	+08.5	+07.5	1.7	0.711	2
63 09 12 Y 05:25	+13.9	+15.3	3.0	0.672	2
64 09 29 Y 05:28	+09.0	+10.7	3.5	0.697	3
64 09 30 Y 06:30	+09.0	+10.7	3.6	0.713	3
64 10 08 Y 03:45	+08.9	+10.9	4.2	0.619	3
65 08 05 Y 08:45	+04.6	+03.2	3.3	0.637	3

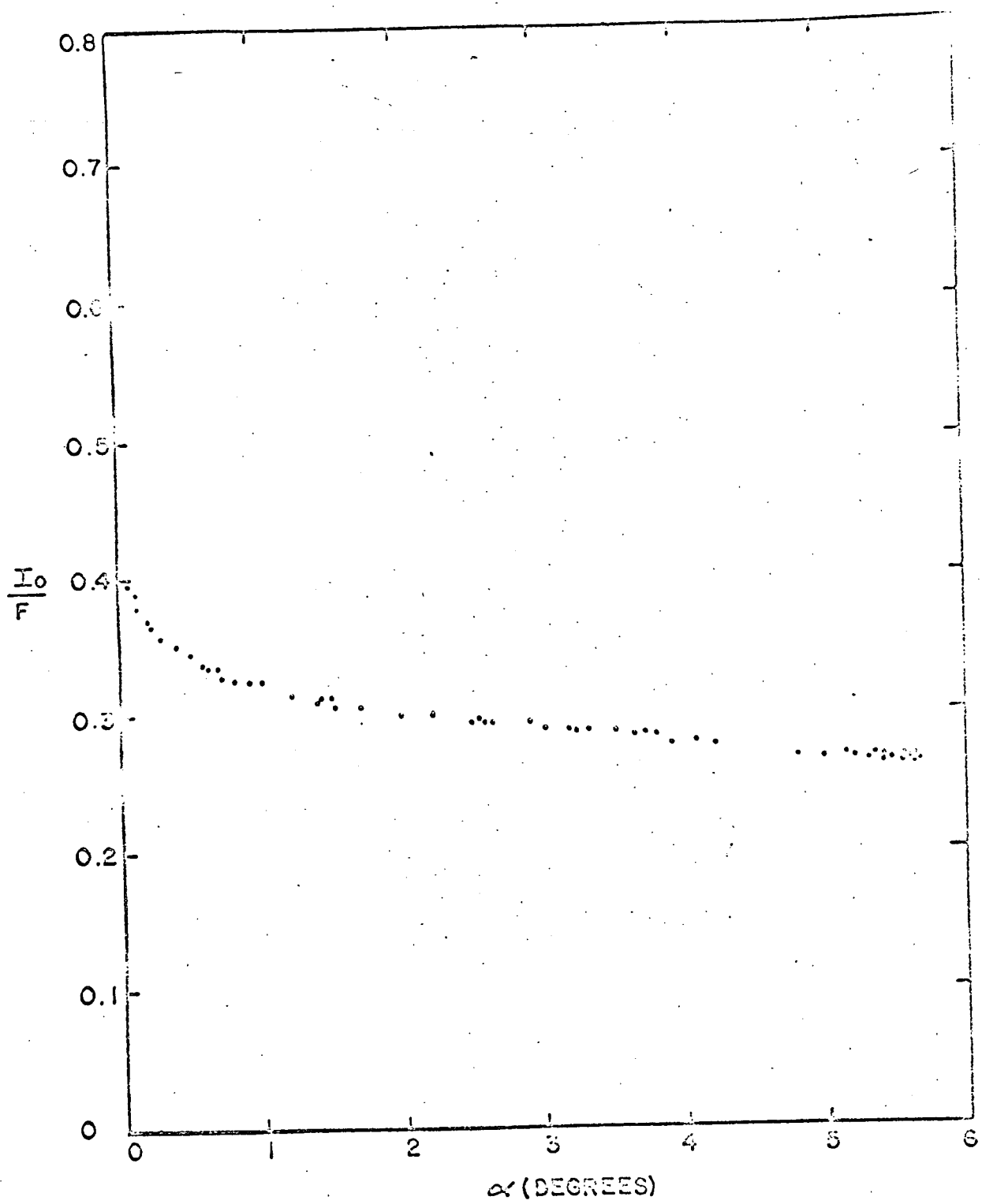
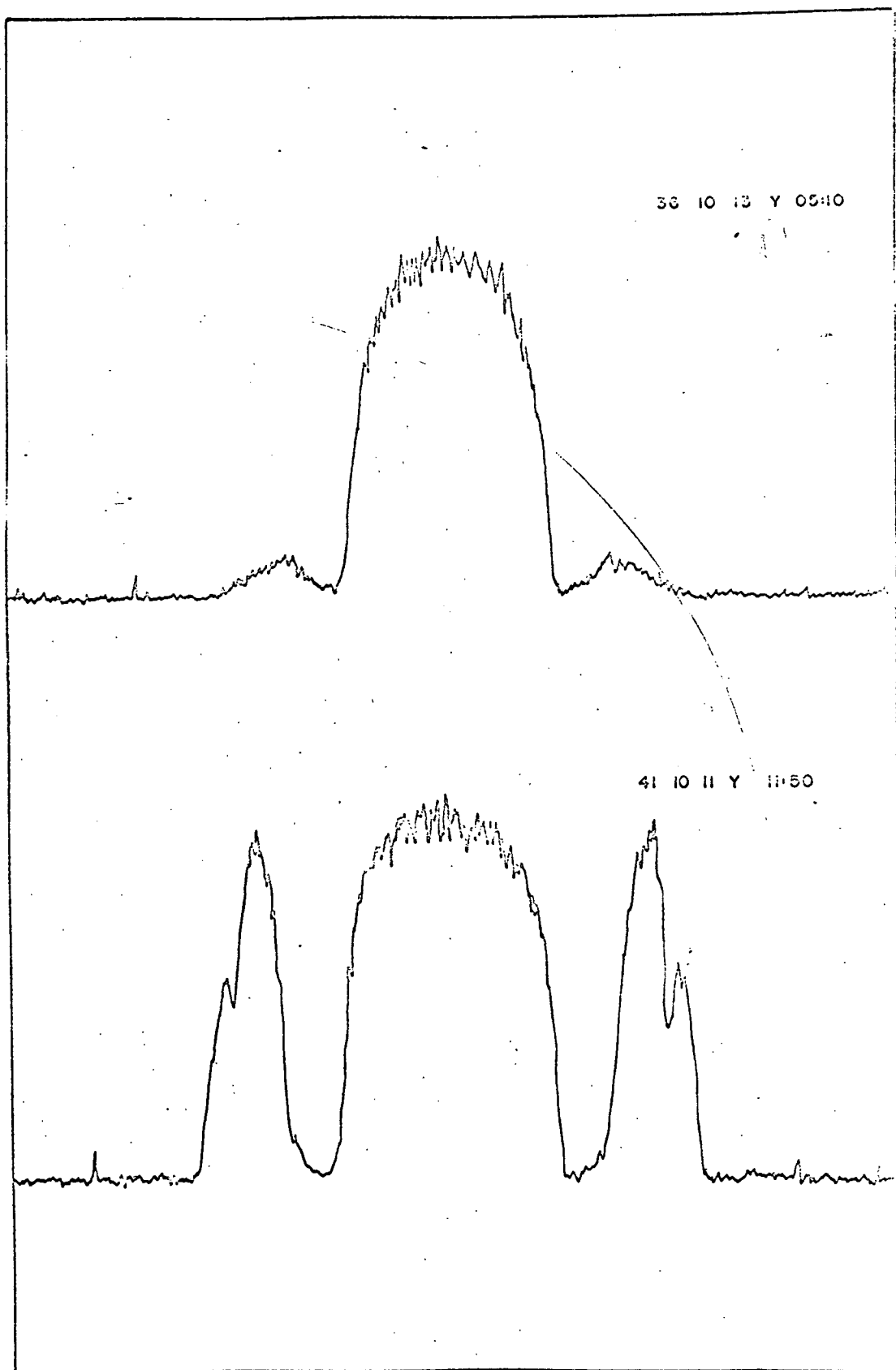


Fig 1.



D

Fig 2

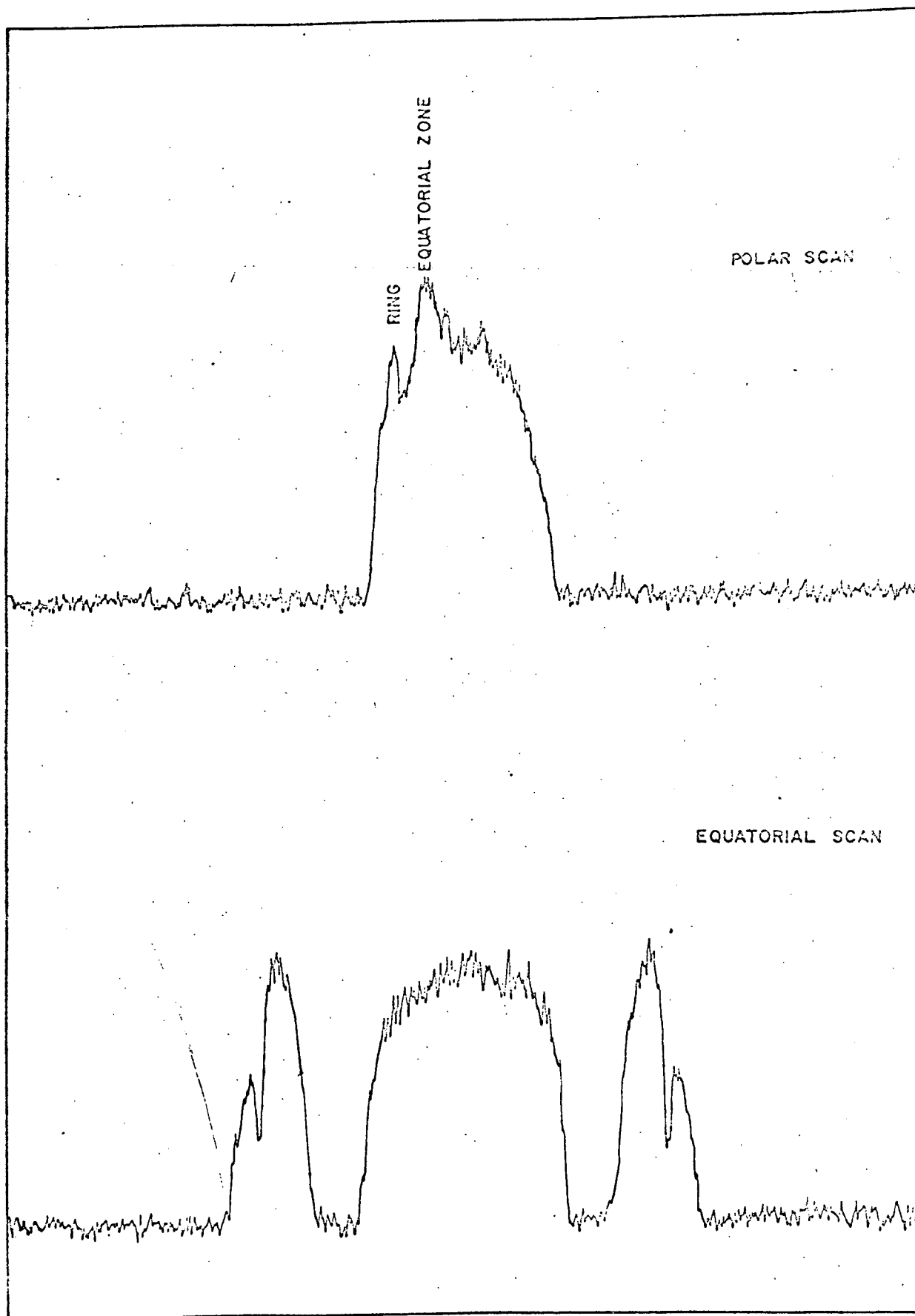


FIG 3

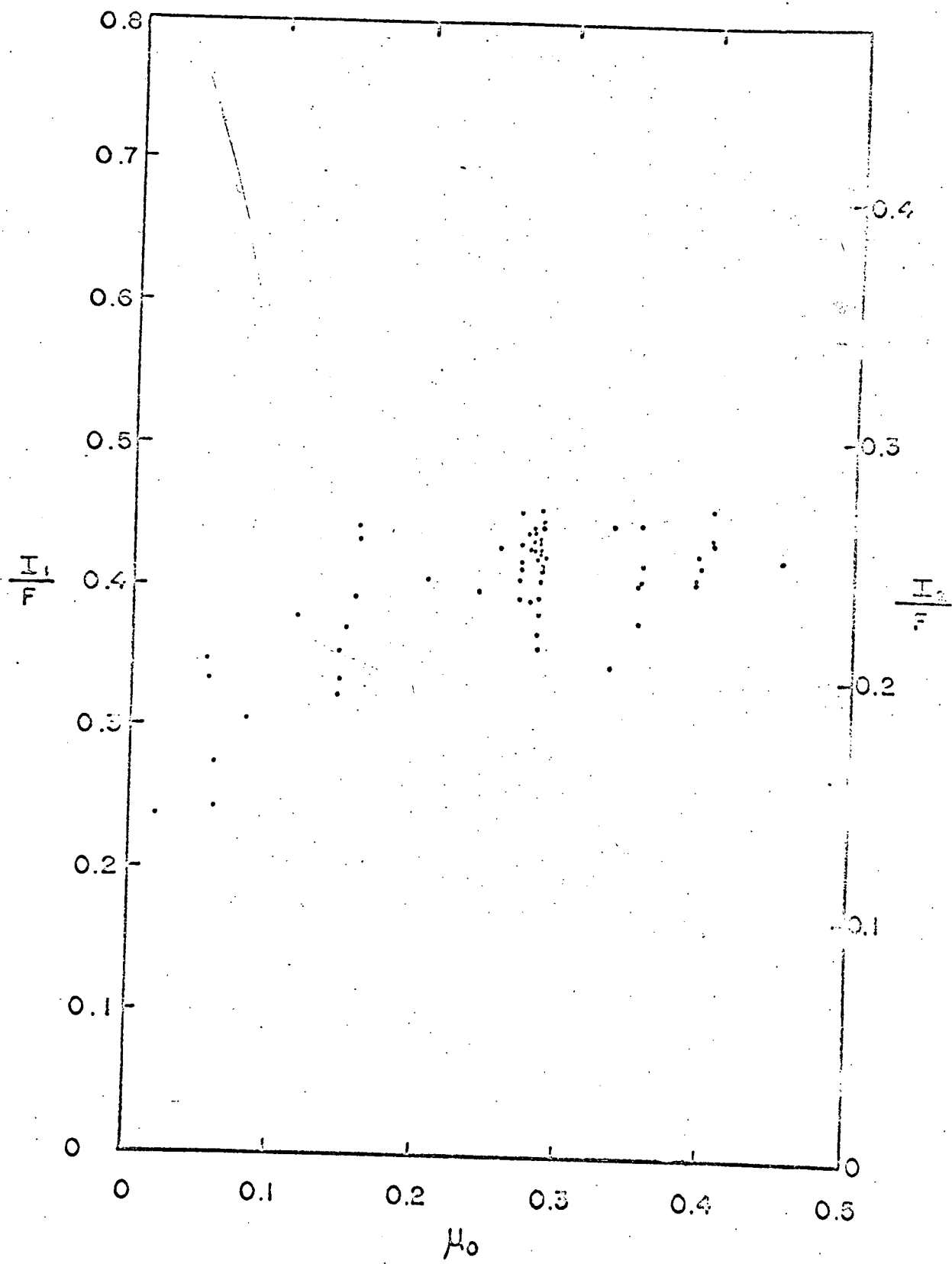
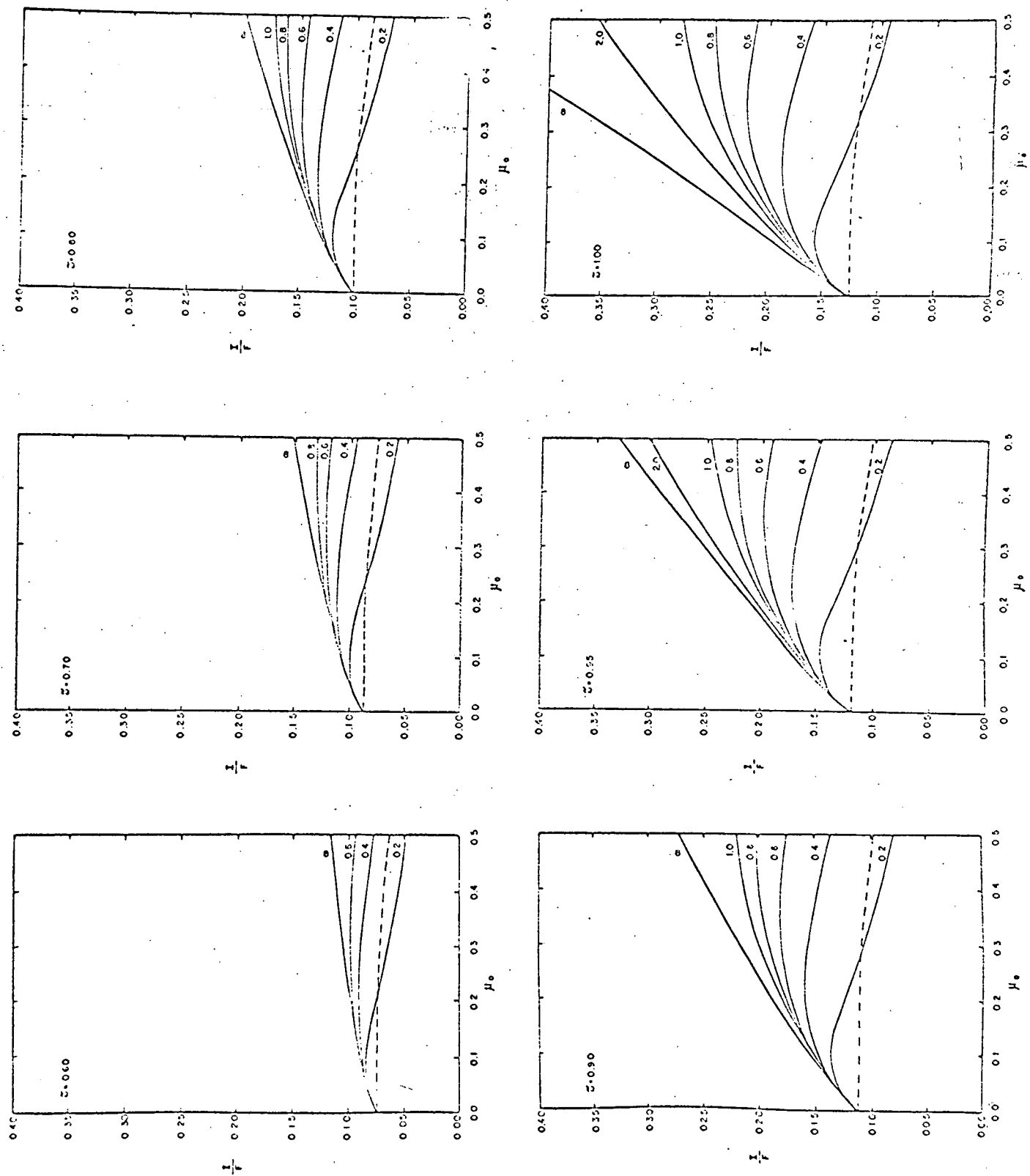


Fig 4

Fig. 61



APPENDIX II

Preprint of paper entitled

"THE PHYSICAL PROPERTIES OF THE JOVIAN ATMOSPHERE
INFERRED FROM ECLIPSES OF THE GALILEAN SATELLITES.
II. 1971 APPARITION"

by

M. J. Price

J. S. Hall

P. B. Boyce

R. Albrecht

Accepted for publication in ICARUS;
Probable publication date 1972 June

IIT RESEARCH INSTITUTE

THE PHYSICAL PROPERTIES OF THE JOVIAN
ATMOSPHERE INFERRED FROM ECLIPSES OF THE
GALILEAN SATELLITES. II. 1971 APPARITION

M. J. Price

Astro Sciences, IIT Research Institute, Chicago, Illinois 60616

and

J. S. Hall, P. B. Boyce, R. Albrecht
Lowell Observatory, Flagstaff, Arizona 86001

Received _____

No. copies submitted: 4

No. MS Pages: 19

No. Figures: 4

No. Tables: 0

Proposed Running Head: ECLIPSES OF THE GALILEAN SATELLITES

Address to which proofs should be sent:

Dr.M.J.Price
Astro Sciences
IIT Research Institute
10 W. 35th St.
Chicago, Illinois
60616

PRECEDING PAGE BLANK NOT FILMED

ABSTRACT

Further simultaneous two-color photoelectric photometry of Ganymede was carried out at blue (λ 4500 Å) and yellow (λ 5790 Å) wavelengths during its eclipse by Jupiter on 1971 March 10. In both colors, the shape of the ingress light curve was again reliably determined for extinctions up to 9 magnitudes. Neither curve showed any evidence of a refraction tail. The observations have been interpreted in terms of the local optical transmission properties of the Jovian atmosphere. At gas number densities $\sim 5 \times 10^{18} \text{ cm}^{-3}$, the maximum photon scattering mean free path at visual wavelengths was 47 km atm. Evidence indicates that neither a simple reflecting-layer model nor a semi-infinite homogeneous scattering model provides an adequate physical description of the atmosphere. Not only is a vertically inhomogeneous scattering model required but, in addition, the scattering mean free path is dependent on "geographical" location, and probably on time also. No unique scattering model exists for the Jovian atmosphere.

Preceding page blank

I. INTRODUCTION

In a recent paper, Price (1970) described a novel technique for inferring the physical properties of the Jovian atmosphere. From a detailed discussion of all observational and theoretical problems involved, he showed that eclipses of the Galilean satellites provide an effective method of monitoring both the physical structure and optical scattering properties of the atmosphere, with excellent resolution in height, latitude, and longitude. Refraction of sunlight through the atmosphere is the physical basis of the technique; multi-color photometry of the satellites throughout ingress provides the observational data needed for the analysis. In principle, not only can the scale height be reliably determined as a function of altitude but, in addition, small quantities of aerosol particles can be detected at high altitudes. Because the atmospheric properties are derived from the shapes of the refraction "tails" to the ingress light curves, accurate photometry down to the lowest light levels is essential.

Initial use of the eclipse technique was made during the spring of 1970. Preliminary results obtained by Price and Hall (1971) were reported in a paper hereinafter referred to as Paper I. Simultaneous two-color photoelectric photometry of Ganymede was carried out at blue (λ 4500 Å) and yellow (λ 5790 Å) wavelengths during its eclipse by Jupiter on 1970 March 24. In both colors, the shape of the ingress light curve was reliably determined for extinctions up to 9 magnitudes using an area-scanning photometer. Both curves showed a refraction tail after the satellite had entered the geometric shadow of the planet. The observations were used

to infer the local, basic optical scattering properties of the atmosphere. At gas number densities near $5 \times 10^{18} \text{ cm}^{-3}$, the atmosphere contains a haze of aerosol particles whose radii are at least 1μ . Their maximum permissible number density was found to be 0.2 cm^{-3} . At both blue and yellow wavelengths the amount of gas in a scattering mean free path was 140 km atm. The results were used to show that neither a simple reflecting-layer model nor a semi-infinite homogeneous scattering model could provide an adequate physical description of the Jovian atmosphere at gas number densities less than 10^{20} cm^{-3} . A vertically inhomogeneous scattering model was indicated. In view of the potential significance of that conclusion for the interpretation of Jovian spectra, confirmation was highly desirable. It was of particular interest to determine if the scattering mean free path depends on "geographical" location and time as well as on altitude. Further eclipse observations were, therefore, carried out during the 1971 apparition of Jupiter. The results are reported in this paper.

II. OBSERVATIONS

Simultaneous two-color, blue ($\lambda 4500 \text{ \AA}$) and yellow ($\lambda 5790 \text{ \AA}$), photometry of Ganymede was carried out during its entry into the Jovian shadow on 1971 March 10. Observations were made using the area-scanning photometer described in detail by Hall (1968), coupled with the 72-inch aperture Perkins reflector of the Ohio State and Ohio Wesleyan Universities at Lowell Observatory. Apart from minor modifications, the equipment was almost identical with that used by Price and Hall (1971). However, the efficiency of the

photometer had been much increased by improvements in the electronic data-handling equipment. All pulses from both photomultipliers were now recorded continuously using a PDP 11 computer. Following integration of any selected number of scans, the data were automatically buffered for subsequent recording on both magnetic and paper tapes. An oscilloscope was used to monitor the integrated scans.

To minimize the problem of scattered light from the nearby planetary disk, we chose to observe the most convenient eclipse of Ganymede which occurred closest to the time of western quadrature of Jupiter (1971 March 23). The optimum eclipse took place on 1971 March 10, midpoint of ingress being predicted by the American Ephemeris and Nautical Almanac for 10:56 UT (03.56 MST). Both Jupiter and Ganymede were then very favorably located for observation from Flagstaff. The elevation angle of the planet was 30° , corresponding to a local hour angle of $1^h 39^m$ and a declination of -20° . Ganymede entered the shadow of Jupiter at an angular distance of 2.3 Jovian radii (about $45''$ of arc) from the limb to the planet. Figure 1 shows the sky location of Ganymede during ingress relative to Jupiter. Additional steps to reduce scattered light included washing the primary mirror, and realuminizing the secondary, immediately prior to the observations. Baffling was placed in the optical system (Cassegrain) of the telescope also. To prevent moonlight from being a problem, the skeleton tube of the telescope was wrapped along its entire length with black cloth.

Reliable photometry at the lowest light levels required that the ratio of the signal-to-sky background noise be maximized. The area scanned was therefore held to a minimum consistent with the area of the satellite image. Bearing in mind both the typical "seeing" quality at Flagstaff and the angular diameter of the satellite, we chose a scan length of 1.5 mm (9".5) and a scan width of 1.08 mm (6".9). Scan length was selected by using an appropriate cam in the scanning mechanism of the photometer; scan width was defined by a slot. The entrance aperture of the photometer was a rectangle of dimensions 6".9 x 0".56, defined by an adjustable slit (selected width 0".56) situated in front of the slot. Such a small slit width could be used because of improvements in the efficiencies of the telescope and photometer. The area scanned is shown in Figure 1.

Throughout ingress, the transparency of the Flagstaff sky was monitored by continuously measuring the brightness of the satellite Callisto in integrated light with the 42-inch reflector immediately adjacent to the Perkins telescope. The transparency was constant to within 1 - 2 percent. The seeing disk of a star, taken to contain 90% of the light, had a diameter varying during the night in the range 1" - 2" of arc. Since the angular diameter of Ganymede is on the order of 2" of arc, the diameter of its seeing disk varied in the range 4" - 6" of arc. During ingress, the Moon, which was nearly full, was setting in the west over 90° from Jupiter. Moonlight did not adversely affect the photometry.

Because the area scanned by the photometer was so

small, it was essential for the telescope to be guided accurately on Ganymede. Off-set guiding on a star was not feasible because of the rapid motion of Jupiter with respect to the stellar background. However, by guiding on one of the other Galilean satellites, total compensation for the motion of Jupiter could be achieved. Moreover, by selecting a satellite on the far side of the planet, moving in towards its limb, most of Ganymede's motion with respect to Jupiter could be guided out. Calculations of the relative motions of the satellites indicated that Callisto was well situated for use as the guide object. During the entire period of ingress (about 20 minutes), Ganymede moved with respect to Callisto by no more than $0''.5$, far less than the diameter of its seeing disk. To minimize the significance of guidance errors, the length of the scanned rectangle was oriented parallel to the direction of drift. With respect to Callisto, Ganymede drifted towards position angle $99^\circ 9'$, c.f., Figure 1.

The brightness of the satellite was measured repeatedly throughout ingress, and an essentially continuous record of the light curve was obtained in both colors. Each brightness measurement consisted of determining the amount of light in each color passing in 15 seconds through the effective aperture of the photometer - the rectangular area of sky scanned. The raw data used were the integrated scans in both colors, obtained by summing groups of 15 successive one-second scans. The brightness was determined by summing the photoelectrons

counted in each integrated scan. The sky backgrounds in the two colors were taken as the means of 35 successive brightness measurements made immediately after the satellite became no longer detectable above the noise level of the sky. The r.m.s. errors of the individual sky brightness measurements were 2.7% and 2.5% for blue and yellow light, respectively. The brightnesses of the uneclipsed satellite (plus sky background) in the two colors were taken as the means of 35 successive measurements made immediately prior to the beginning of ingress. The r.m.s. errors of these individual brightness measurements were 2.7% and 4.6% for blue and yellow light, respectively.

The observed light curves, in blue and yellow light, are shown in Figures 2 and 3, respectively. Extinction in magnitudes is plotted against time in seconds. The zero point in time is set at the interpolated half-intensity point. The time resolution was 15.6 seconds. Each individual brightness measurement was located in time to an accuracy of ± 0.5 seconds. In both figures, the plotted points have been normalized assuming zero extinction outside eclipse. The final data point refers to the minimum measurable brightness when the satellite was barely detectable against the sky background noise. This limit was taken as the individual r.m.s. error of the 35 measurements which define the sky background. In both colors, reliable measurements of the brightness of the satellite were made down to extinctions of 9 magnitudes.

The photometry contained both systematic and random errors. Systematic errors resulted from the use of a short

slit (6"9) as the entrance aperture of the photometer. Because of seeing effects, a small fraction of the light from the satellite spilled over each side of the scanned rectangle. During ingress unpredictable changes in the size of the satellite image caused systematic errors in the photometry, both colors being affected nearly equally and simultaneously. By comparison, errors resulting from imperfect guiding and differential refraction were insignificant. The systematic errors are readily apparent in Figures 2 and 3. Initially, it was thought that the structure in the observed light curves might have originated in the particular distribution of reflectivity over the disk of the satellite. That idea was discarded, however. Simultaneous photometry of the eclipse, carried out by Greene, Shorthill, and Despain (1971) with the 200-inch Palomar reflector, using a circular aperture of 14" of arc diameter, showed no such structure. Random errors resulted from scintillation of the satellite image, and from the statistics of photon counting. Scintillation effects dominate for extinctions less than 7 magnitudes. In the fainter regions of the light curves, poor photon counting statistics, caused by a low ratio of signal-to-sky background noise, limit the accuracy of the measurements. Neglecting systematic effects, the net r.m.s. errors in each brightness measurement are indicated in Figures 2 and 3 by the vertical bars attached to each plotted point. In the faintest regions of the light curves the error reaches 100%.

III. ANALYSIS

Interpretation of the observational data required the calculation of two-color ingress light curves for a range of models of the Jovian atmosphere. Our calculations followed exactly the theory described in Paper I. Both clear (gaseous) and hazy (aerosol) atmospheric models were used. Selection of their fundamental parameters was discussed in Paper I. The clear model assumed the atmosphere to consist of a homogeneous, isothermal layer of molecular hydrogen and helium lying above a sharply defined, dense cloud layer. On the basis of current knowledge, the H_2/He ratio by numbers was taken as 5.1, the temperature of the gas as $145^\circ K$, the corresponding scale height as 20.8 km, and the pressure at the cloud tops as 2.02 atmospheres. The haze models assumed the atmosphere to be semi-infinite, composed of a homogeneous mixture of aerosol particles and gas. Each hazy model used the same basic parameters as the clear model. Now, however, instead of the reference level being the top of a sharply defined cloud layer, we assume it is the effective depth to which visual continuum solar photons penetrate at normal incidence. Application of the theory demands a knowledge of the photometric radius of the satellite, obtainable by studying the general shape of the brighter regions of each ingress light curve. In spite of the seeing structure apparent in the observed curves, the theoretical curves were in satisfactory agreement over an extinction range of 5 magnitudes when a satellite radius

of 2100 (± 100) km was used. The optimum photometric radius agreed well with the corresponding value (2200 km) derived in Paper I.

In the clear model, sunlight being refracted through the atmosphere suffers attenuation by both differential refraction and Rayleigh scattering. In the hazy models, additional opacity results from scattering and absorption by the aerosol particles. To quantify the aerosol opacity, we use a haze parameter defined as the ratio of the total extinction cross-section to the effective Rayleigh scattering cross-section for the H_2 -He mixture alone. Two-color ingress light curves were calculated for haze parameters ranging from unity (clear) through 30 (optically thick). For λ 4500 Å, increasing the haze parameter beyond 10 produced negligible change in the computed refraction tail; for λ 5790 Å, the corresponding value for the haze parameter was 20.

In Figures 2 and 3, the main theoretical results are compared with the observations. It is immediately apparent that neither of the observed light curves shows any trace of a refraction tail. Consequently, only a minimum value for the haze parameter at each wavelength can be obtained. To account for the observations, we require the haze parameter to have minimum values of 5 and 10 for blue and yellow light, respectively. The effective Rayleigh scattering cross-sections of the gas mixture are $1.88 \times 10^{-27} \text{ cm}^2$ at λ 4500 Å and $6.65 \times 10^{-28} \text{ cm}^2$ at λ 5790 Å; the minimum total extinction cross-sections are $9.4 \times 10^{-27} \text{ cm}^2$ and $6.7 \times 10^{-27} \text{ cm}^2$,

respectively. For convenience, we will use $8.0 \times 10^{-27} \text{ cm}^2$ as the minimum total extinction cross-section for both colors. Lack of detectable refraction tails in both colors is consistent with the aerosol particles having radii greater than $\sim 1 \mu$.

Interpretation of the total extinction cross-section in terms of the photon scattering mean free path requires a knowledge of which atmospheric strata are responsible for the refraction tail. Since these strata are very nearly the same for both blue and yellow light, we need consider only one color. The necessary information for yellow light is contained in Figure 4. Three quantities are plotted as a function of time, measured from the midpoint of ingress; first, the height, h_c , above the reference level in the atmosphere for a ray of light joining the centers of the solar and satellite disks at its closest approach to the center of the planet; second, the corresponding number density, $N(h_c)$, of gas molecules; third, the height resolution, Δh , permitted by the envelope of rays joining the solar and satellite disks. Comparison of Figures 3 and 4 shows that the regions of the atmosphere probed at the end of ingress correspond to gas number densities near $5 \times 10^{18} \text{ cm}^{-3}$.

To compare the optical properties of the Jovian atmosphere derived in this paper with those reported in Paper I, we require information concerning which "geographical" regions were probed. Because of the large negative planetocentric declination of the sun ($-3^\circ 03'$), the region of the

Jovian atmosphere probed during ingress of Ganymede on 1971 March 10 was located at a high southerly latitude, midpoint of ingress corresponding to a longitude of 231° (System II) and a latitude of -56° . By comparison, the region probed during ingress of Ganymede on 1970 March 24 was located at a longitude of 335° (System II) and a latitude of -53° . Note the errata in Paper I. For both eclipses, the resolution achieved in longitude was $\sim 4^\circ$, in latitude $\sim 3^\circ$, c.f. Price (1970).

The minimum value for the total extinction cross-section at visual wavelengths may be used to determine a minimum value for the optical path traversed by the refracted sunlight, together with a maximum value for the photon scattering mean free path. Following Price (1970), we can write the total number of gas molecules per cm^2 , N_t , in the refraction path through the atmosphere as equal to $(2\pi RH)^{1/2} N_g$, where N_g is the number density of gas molecules in the region of the atmosphere responsible for the refraction, R is the radius of Jupiter, and H is the scale height. Since N_g is on the order of $5 \times 10^{18} \text{ cm}^{-3}$, R is $7.135 \times 10^4 \text{ km}$, and H is 20.8 km , we obtain a value of N_t equal to $1.52 \times 10^{27} \text{ cm}^{-2}$. It follows that the minimum optical path length traversed by the refracted sunlight is 12.2 for both blue and yellow light. The maximum number of molecules per photon scattering mean free path is therefore $1.25 \times 10^{26} \text{ cm}^{-2}$, equivalent to 47 km atm. Comparing our

estimate of the maximum scattering mean free path with the measured value reported in Paper I, we conclude that the local concentration of aerosol particles in the Jovian atmosphere is variable. At gas number densities $\sim 5 \times 10^{18} \text{ cm}^{-3}$, the concentration varies by at least a factor 3 with "geographical" position, and possible with time also.

International Planetary Patrol photographs of Jupiter taken on or near 1970 March 24 and 1971 March 10 were studied to determine if there were any obvious differences in the cloud structure in the "geographical" regions scanned during each eclipse of Ganymede. None was found. For the 1970 eclipse, the latitude of -53° lay within a transition zone from the South Temperate Zone (STeZ) to the South Polar Region (SPR). The latitude region from -50° to -70° was generally dark. For the 1971 eclipse, the latitude of -56° lay within the South Polar Region (SPR), a dark feature of the Jovian disk.

IV. CONCLUDING REMARKS

In Paper I, we concluded that the optical properties of the Jovian atmosphere should be discussed in terms of a vertically inhomogeneous scattering model. Our analysis in this paper indicates that the local scattering mean free path is dependent on "geographical" location, and probably on time also. We conclude that no unique scattering model exists for the Jovian atmosphere. Further application of the eclipse technique is warranted.

ACKNOWLEDGMENTS. It is a pleasure to thank Miss Louise A. Riley for assistance at the Perkins telescope, N. White for using the adjacent 42-inch reflector to monitor the sky transparency during the course of our observations, K. Williams for computer-processing the raw observational data, and observers from the Ohio State and Ohio Wesleyan Universities for co-operation in scheduling telescope time. We would also like to thank T.F. Greene, R.W. Shorthill, and L. G. Despain for providing access to their observational data prior to its publication; C.F. Capen for providing information from the International Planetary Patrol Program concerning the appearance of Jupiter during the 1970 and 1971 apparitions; and N. U. Mayall for generously providing access to the facilities of the Computer Laboratory at Kitt Peak National Observatory for the initial analysis of the observational data. Kitt Peak National Observatory is operated by the Association of Universities for Research in Astronomy, Inc., under contract with the National Science Foundation. This research was sponsored by the National Aeronautics and Space Administration under contract NASW-2257. Partial support was also provided by Lowell Observatory under NASA grant NGR-03-003-001, and by IITRI as In-house project V1069.

REFERENCES

- Greene, T.F., Shorthill, R.W., and Despain, L.G. (1971).
Private communication.
- Hall, J.S. (1968). A scanning polarimeter. Lowell Obs. Bull.
7, 61-66.
- Price, M.J. (1970). On the inference of the physical properties of the Jovian atmosphere from photometry of eclipses of the Galilean satellites. NASA Technical Report R-345, USGPO, Washington.
- _____ and Hall, J.S. (1971). The physical properties of the Jovian atmosphere inferred from eclipses of the Galilean satellites. I. Preliminary results. *Icarus*. 14, 3-12.

FIGURE CAPTIONS

Figure 1. Relative sky locations of Jupiter and Ganymede during shadow ingress on 1971 March 10. The scanning aperture of the photometer is the solid rectangle adjacent to Ganymede. The direction of scan was oriented parallel to the drift direction of Ganymede with respect to Callisto. For convenience, the oblateness of Jupiter has been neglected. Moreover, the image of Ganymede is shown unbroadened by "seeing" effects.

Figure 2. The ingress light curve, at an effective wavelength of 4500 \AA , for the eclipse of Ganymede on 1971 March 10; comparison of theory with observation.

Figure 3. The ingress light curve, at an effective wavelength of 5790 \AA , for the eclipse of Ganymede on 1971 March 10; comparison of theory with observation.

Figure 4. The regions of the Jovian atmosphere responsible for the extinction of the refraction tail to the ingress light curve, at an effective wavelength of 5790 \AA , for the eclipse of Ganymede on 1971 March 10. Mid-ingress (half-intensity point) corresponds to a planetocentric longitude (System II) of 231° and a latitude of -56° . Three quantities are plotted as a function of time, which is measured from the midpoint of ingress; first, h_c , the height above the reference level in the atmosphere for a ray of light joining the centers of the solar and satellite disks at its closest approach to the center of the planet; second, $N(h_c)$, the corresponding number density of gas molecules;

third, Δh , the height resolution permitted by the envelope of rays joining the solar and satellite disks.

POSITION ANGLE
OF
N. JOVIAN POLE

N. CELESTIAL POLE

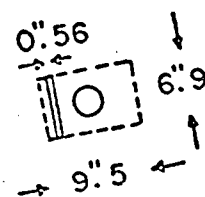
9°.9

EAST

WEST

SOUTH

GANYMEDE (+AREA PHOTOMETERED)



DIRECTION
OF
SCAN

10"

Fig. 1

EXTINCTION (MAGNITUDES)

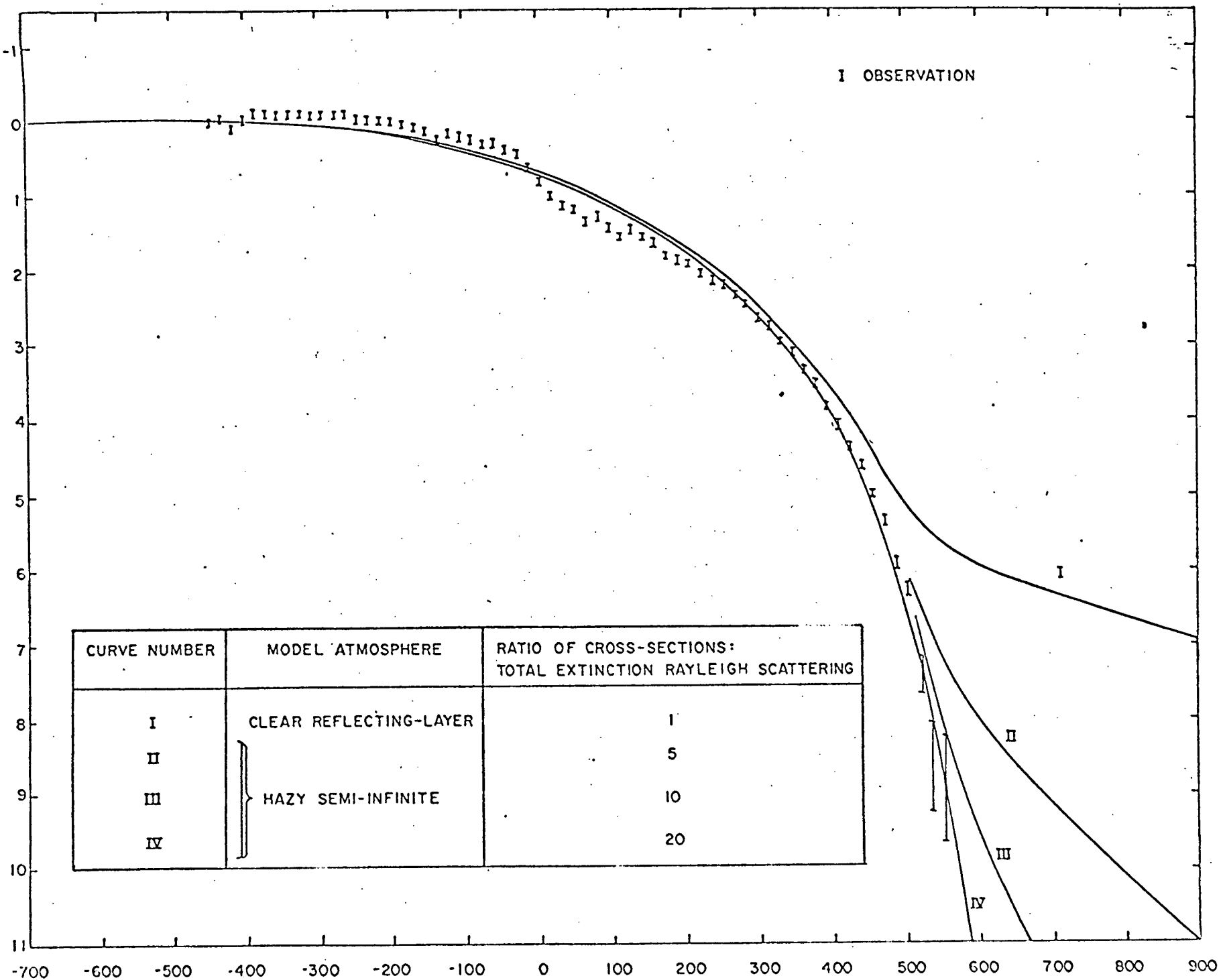
I OBSERVATION

CURVE NUMBER	MODEL ATMOSPHERE	RATIO OF CROSS-SECTIONS: TOTAL EXTINCTION/RAYLEIGH SCATTERING
I	CLEAR REFLECTING-LAYER } HAZY SEMI-INFINITE	1
II		2
III		5
IV		10

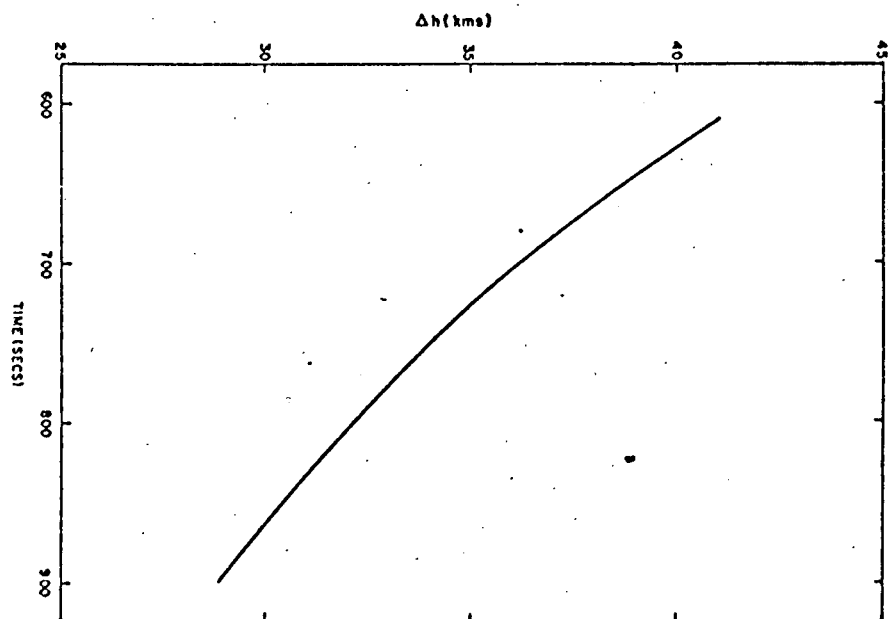
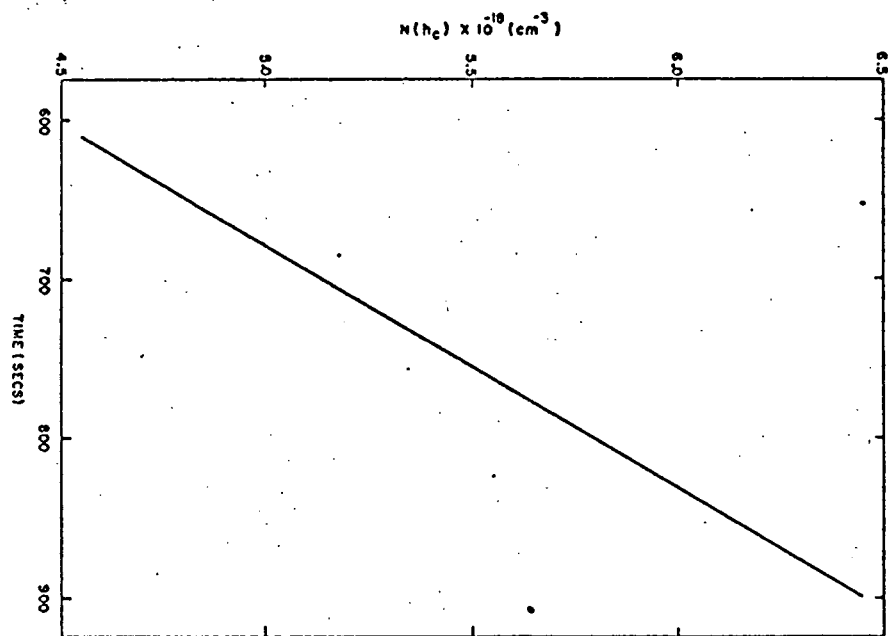
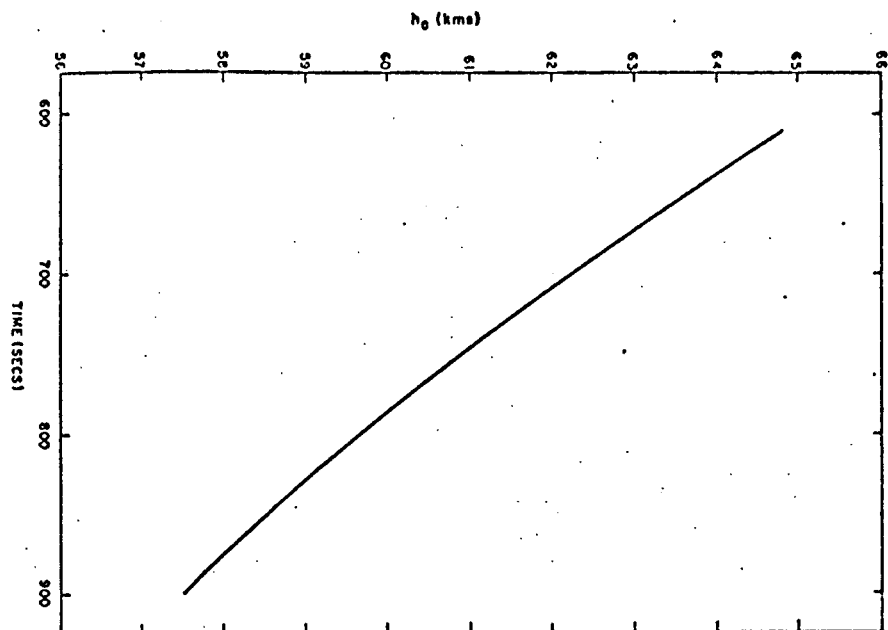
TIME (SECS)

I OBSERVATION

CURVE NUMBER	MODEL ATMOSPHERE	RATIO OF CROSS-SECTIONS: TOTAL EXTINCTION RAYLEIGH SCATTERING
I	CLEAR REFLECTING-LAYER	1
II	HAZY SEMI-INFINITE	5
III		10
IV		20



7-11



APPENDIX III

Preprint of paper entitled
"PHOTOMETRIC RADII OF IO AND EUROPA"

by
M. J. Price
J. S. Hall
P. B. Boyce
R. Albrecht

Published on 1971 November 2
as

LOWELL OBSERVATORY BULLETIN NO. 156
Vol. VII, No. 19, pp. 207-210, 1971

IIT RESEARCH INSTITUTE

PHOTOMETRIC RADII OF IO AND EUROPA

M. J. Price*, J.S. Hall, P. B. Boyce, and R. Albrecht

During the 1970 and 1971 apparitions of Jupiter, multi-color photometric observations of eclipses of the Galilean satellites were carried out at Lowell Observatory in a research program designed specifically to infer the physical structure and optical scattering properties of the planetary atmosphere. In essence, the brighter region of the ingress light curve is used to obtain an optimum photometric radius for the satellite; the refraction tail is then interpreted in terms of the optical properties of the Jovian atmosphere. All aspects of the eclipse technique have been fully discussed by Price (1970). In addition, two successful applications based on eclipses of Ganymede have been reported by Price and Hall (1971) and by Price, et al. (1972). During the program, observations of the ingress light curve of Io and Europa were also made. These data have been analyzed to obtain photometric radii for both satellites. This paper briefly reports the observations and their interpretation. The results are compared with satellite radii obtained using other observational techniques.

Simultaneous two-color photoelectric photometry of Io and Europa was carried out during their eclipse by Jupiter on the night of 1971 April 5/6. Ingress observations at blue

*Visiting Astronomer. Permanent affiliation: Astro Sciences, IIT Research Institute, Chicago, Illinois.

(λ 4500 Å) and yellow (λ 5790 Å) wavelengths were made using a two-channel area-scanning photometer, described in detail by Hall (1968), coupled with the 72-inch aperture Perkins reflector of the Ohio State and Ohio Wesleyan Universities. The observational procedures, the electronic recording equipment, the method of reducing the data to obtain the ingress light curves, the analysis of the photometric errors, and the interpretation of the results in terms of the photometric radii of the satellites, all were exactly as described by Price, et al. (1972).

Figures 1 and 2 show the observed two-color ingress light curves for Io at blue and yellow wavelengths, respectively. The corresponding data for Europa are shown in Figures 3 and 4. For both eclipses, the integration time used to obtain each data point (i.e., the time-resolution) was 10.4 seconds. For Io, the shapes of the pair of ingress light curves were reliably determined for extinctions up to 5 magnitudes. For Europa, reliable data were obtained for extinctions up to 7.5 magnitudes. Also shown are theoretical light curves computed on the assumption that Jupiter has no atmosphere above a sharply defined dense cloud layer; the ball was taken to have a "hard" surface. Best agreement between theory and observation was obtained by using radii of 1650 km and 1450 km for Io and Europa, respectively. Both radii are estimated to be uncertain by ± 100 km.

Previous attempts have been made to infer the satellite radii from eclipse photometry. Photographic

observations were initiated at the Harvard Observatory in 1878 by Pickering (1907). By comparison with our own set of measurements, the observed ingress light curves were imprecisely defined. Sampson (1909) analyzed the available photometric data to obtain radii for Io and Europa of 1700 km and 1500 km, respectively. Both values are consistent with our own results. Using photoelectric photometry at visual (yellow) wavelengths, Harris (1961) and Kuiper obtained more accurate ingress light curves. In their analysis, they adopted radii of 1620 km and 1430 km for Io and Europa, respectively. Agreement between theory and observation was not, however, entirely satisfactory. For Io, the most consistent agreement was obtained after increasing the adopted radius by 14 percent to 1850 km. The results obtained by Harris and Kuiper agree moderately well with our own.

Several more direct techniques have been used to measure the radii of the satellites. Camichel (1953) determined radii by comparing images of the satellites with artificial disks projected in the field of a telescope. The disks were of adjustable size, brightness, color, and limb-darkening. Dollfus (1954) also measured the radii with a double-image micrometer. The two sets of measurements agree around the following values: Io, 1775 km; Europa, 1550 km.

Interferometric measurements of the satellite radii have been made by Michelson (1891a, b), who used a double-slit device in front of the objective of a 12-inch aperture

refracting telescope. These observations were repeated by Hamy (1899), who used a similar technique but with larger slits to increase the luminosity of the image. Measurements have also been made by Danjon (1936), who used a half-wave interference micrometer. Systematic differences appear between the radii obtained by each observer. Radii measured by Danjon are systematically smaller than those obtained by Hamy; those measured by Michelson are the smallest. Even so, by using an improved reduction technique, Danjon (1945) succeeded in reconciling the different interferometric measurements to an accuracy of ± 5 percent. Basic assumptions in his analysis were that each satellite is spherical, and that its disk is uniformly reflective. His analysis gave the following mean radii: Io, 1650 km; Europa, 1450 km.

Filar micrometric measurements of the radii of the satellites have been made by many observers. In particular, Barnard (1895) used the Lick 36-inch aperture refractor to make an excellent set of measurements. He obtained the following values for the radii: Io, 1973 ± 30 km; Europa, 1646 ± 41 km. Barnard compared his results with the mean values obtained from 9 sets of similar observations made by 9 different observers. His results agree closely with those values. Further measurements by Dyson (1895) agree closely with the results obtained by Barnard.

But by far the most accurate method for obtaining the radii of the satellites is to utilize their rare stellar occultations. On 1971 May 14, Io occulted the star

β^2 Scorpii. Worldwide observations of the event have been interpreted by van Flandern (1971) in terms of the dimensions of the satellite. Io appears to be spherical to an accuracy of ± 1 km, its mean diameter being 3654.8 ± 4.6 km. Within its estimated accuracy, the prior determination of the radius of Io made using the eclipse technique agrees satisfactorily with the occultation result. No stellar occultations by Europa have yet been observed. According to O'Leary (1971) favorable occultations are relatively rare.

Table I summarizes the measurements of the radii of Io and Europa obtained using the different techniques available. We conclude, primarily on the basis of the 1971 stellar occultation result, that the eclipse technique can be used to infer satellite radii accurate to ± 10 percent. In principle, the eclipse technique can also be applied to the satellites of Saturn, Uranus, and Neptune for early objective determinations of their radii.

Acknowledgments: It is a pleasure to thank K. Bern for monitoring the transparency of the sky during the course of the observations. This research was supported in part by the National Aeronautics and Space Administration under grant NGR-03-003-001 awarded to the Lowell Observatory, and also under contract NASW-2257 awarded to the IIT Research Institute.

REFERENCES

- Barnard, E.E. (1895) Mon.Not.Roy.Astron.Soc., 55, 382.
- Camichel, M. (1953) Ann.d'Astrophys., 16, 41.
- Danjon, A. (1936) Ann.Obs.Strasbourg, III-4, 181.
- _____. (1945) Ann.d'Astrophys., 7, 135.
- Dollfus, A. (1954) Comptes Rendus, 238, 1475.
- Dyson, F. (1895) Mon.Not.Roy.Astron.Soc., 55, 477.
- Flandern, T.C. van (1971) Results reported at the 135th Meeting of the Amer.Astron.Soc., held at Amherst, Mass., 1971 Aug. 24-27.
-
- Hall, J.S. (1968) Lowell Obs. Bull. 7, 61.
-
- Hamy, M. (1899) Bull. Astron. 16, 257.
- Harris, D.L. (1961) in "Planets and Satellites", ed. G.P. Kuiper and B.M. Middlehurst, Univ.Chicago Press, p.327.
- Michelson, A.A. (1891a) Pub.Astron.Soc.Pacific, 3, 274.
- _____. (1891b) Nature, 45, 160.
-
- O'Leary, B. (1971) Paper presented at the 135th Meeting of the Amer.Astron.Soc., Amherst, Mass., 1971 August 24-27.
-
- Pickering E.C. (1907) Harvard Ann., vol.52, part 1.
- Price, M.J. (1970) NASA Technical Report R-345, USGPO, 57pp.
- _____ and Hall, J.S. (1971) Icarus, 14, 3.
- _____, Hall, J.S., Boyce, P.B., and Albrecht, R. (1972) Icarus (in press).
- Sampson, R.A. (1909) Harvard Ann., vol.52, part 2.

TABLE I
SUMMARY OF PUBLISHED RADII FOR IO AND EUROPA

Method	Io (km)	Europa (km)	Author	Date	Remarks
Eclipse (photographic)	1700	1500	Sampson	1909	Analysis of existing data.
Eclipse (photoelectric)	1620	1430	Harris, Kuiper	1961	Better agreement for Io if 1850 km used.
Eclipse (photoelectric)	1650	1450	Price, et al.	1971	Scanning used to evaluate sky background continuously.
Stellar Occultation (photoelectric)	1827	----	van Flandern, et al.	1971	By far the most accurate method.
Direct (interferometric)	1650	1450	Michelson	1891	Two slits in front of objective.
			Hamy	1899	As above but larger slits.
			Danjon	1936	Half-wave micrometer.
Direct (visual)	1775	1550	Camichel	1953	Comparison disks.
			Dollfus	1954	Double image micrometer.
	1973	1646	Barnard, et al.	1895	Filar micrometer - ten observers.

FIGURE CAPTIONS

Figure 1. The ingress light curve, at an effective wavelength of 4500 \AA , for the eclipse of Io on 1971 April 6; comparison of theory with observation. The data are represented by the series of vertical bars, their lengths corresponding to the r.m.s. photometric errors. The theoretical curve was calculated for the case of no atmosphere on Jupiter, and a satellite radius of 1650 km.

Figure 2. The ingress light curve, at an effective wavelength of 5790 \AA , for the eclipse of Io on 1971 April 6; comparison of theory with observation. The data are represented by the series of vertical bars, their lengths corresponding to the r.m.s. photometric errors. The theoretical curve was calculated for the case of no atmosphere on Jupiter, and a satellite radius of 1650 km.

Figure 3. The ingress light curve, at an effective wavelength of 4500 \AA , for the eclipse of Europa on 1971 April 6; comparison of theory with observation. The data are represented by the series of vertical bars, their lengths corresponding to the r.m.s. photometric errors. The theoretical curve was calculated for the case of no atmosphere on Jupiter, and a satellite radius of 1450 km.

Figure 4. The ingress light curve, at an effective wavelength of 5790 \AA , for the eclipse of Europa on 1971 April 6; comparison of theory with observation. The data are represented by the series of vertical bars, their lengths

corresponding to the r.m.s. photometric errors. The theoretical curve was calculated for the case of no atmosphere on Jupiter, and a satellite radius of 1450 km.

B

